Journal of Radioanalytical and Nuclear Chemistry
https://doi.org/10.1007/s10967-024-09803-0

Applicability of atomic force microscopy for nuclear forensic examination

Csaba Tóbi[1,2] · Nguyen Quoc Khánh[3] · Zoltán Homonnay[4] · Éva Széles[2]

Received: 5 August 2024 / Accepted: 24 September 2024

Abstract

The applicability of the Atomic Force Microscopy (AFM) was examined for nuclear forensic purposes. The hyper-stoichiometric form of uranium-oxide was identified as novel signature which indicates the production technology of uranium fuel pellets. The AFM technique was compared with Scanning Electron Microscope (SEM) that is usually used for morphological study in nuclear forensics. AFM has some unique features comparing with SEM and as a fast and less expensive technique, it can be a good alternative solution or a supporting technique to the SEM.

Graphical abstract

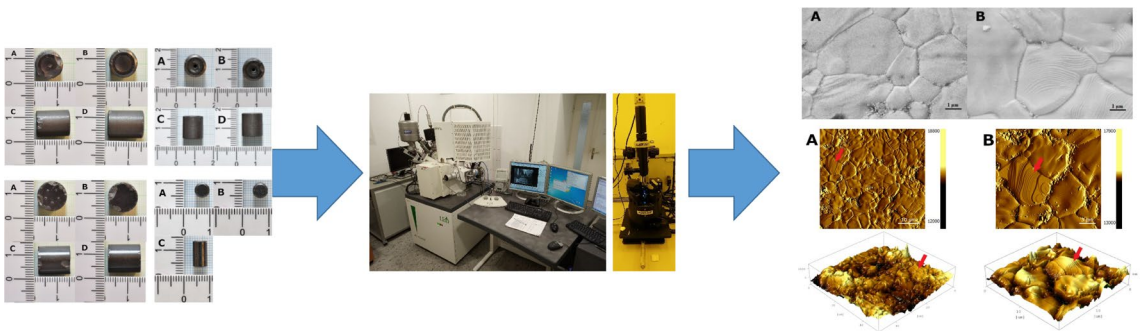

Keywords Atomic force microscopy · Hyper-stoichiometry · Nuclear fuel pellet · Morphology study · Nuclear forensics

Introduction

"Nuclear forensics is the examination of nuclear or other radioactive material, or of evidence contaminated with radionuclides, in the context of legal proceedings under international or national law related to nuclear security" as defined by the International Atomic Energy Agency [1]. This examination is based on analysis of special characteristic parameters of nuclear and other radioactive materials originating from the production technology and application. These characteristic parameters—also known as nuclear forensic signatures—can help to identify the origin and history of confiscated nuclear materials with unknown origin

✉ Csaba Tóbi
tobi.csaba@ek-cer.hu

1 Hevesy György PhD School of Chemistry, Eötvös Loránd University, Pázmány Péter Str. 1/A, Budapest 1117, Hungary

2 Nuclear Security Department, HUN- REN Center for Energy Research, Konkoly-Thege Str. 29-33, Budapest 1121, Hungary

3 Institute of Technical Physics and Materials Science, HUN-REN Centre for Energy Research, Budapest, Hungary

4 Institute of Chemistry, Eötvös Loránd University, Pázmány Péter Str. 1/A, Budapest 1117, Hungary

Published online: 04 October 2024

by the determination of the production technology, production date, isotopic composition and other essential parameters. One of the key signatures is the material morphology that can be easily used for origin assessment [1, 2]. Several scientific studies focusing on the determination and analysis of morphological signatures of nuclear materials can provide valuable information on the origin and the process history of the subject sample [3–5]. For example, the particle morphology of nuclear materials produced and used in the nuclear fuel cycle can be influenced by the parent material (e.g. in the case of uranium ore concentrates, based on the chemical procedure used for production) and the applied physical (e.g. milling, heat treatment…etc.) and/or chemical processes (e.g. precipitation, extraction…etc.) [6].

Characteristic properties related to the morphology of uranium oxide connected to its chrystalic structure. Uranium dioxide crystallises in fluorite structure. One of the special abilities of the material is able to adapt to variable stoichiometry, depending on pressure and temperature. Uranium dioxide exists in stoichiometric (UO_2), hypo-stoichiometric (UO_2-x) and hyper-stoichiometric form (UO_2+x) [7]. "In the case of hypo-stoichiometric oxides ($x<0$) vacancies in the normal oxygen sites are preponderant, on the other hand in the hyper-stoichiometric region ($x>0$) the oxygen-excess atoms are accommodated in octahedral interstitial sites. Such feature is allowed by the presence of a partially filled 5f shell in uranium and the possibility for a U atom to shift easily among the valances $+3, +4, +5$, or $+6$ [8]." The excess oxygen atoms appear as interstitial defects, which are partially ordered. The excess oxygen atoms dynamics and positions are able to control, such as thermal conductivity, fission-product accommodation and transport, micro-structure evolution and corrosion behaviour [9].

The morphological signatures can be examined using different microscopic techniques using visible light, electrons or X-ray for the analysis. To determine the physical, chemical and structural properties of different materials, the following techniques can be used: Optical Microscopy (OM), Scanning Electron Microscopy (SEM), Transmission Electron Microscopy (TEM), Electron Microprobe Analysis (EMA), X-ray Microanalysis (XRM) and Optical Spectroscopy (OS) [10].

Based on the scientific publications in the case of nuclear forensic examination, the most commonly used technique is SEM. The reason of the popularity of SEM is that the technique can achieve a higher resolution and magnification in images than the Optical Microscopy and with the combination of Energy-dispersive X-ray spectroscopy, it can also able to determine elemental composition of the sample. The image quality is also important in the case of nuclear materials, especially e.g. uranium ore concentrates or uranium oxide powders, where a 5–10 nm thin conductive layer must be formed (e.g. Au, Pd, C) on the sample before SEM measurement to avoid surface charging. Furthermore, in this way particles can also be fixed on the surface, so will not be repelled off during the scanning with the electron beam [10–12].

Atomic Force Microscopy uses a very sharp probe (tip) mounted on the microcantilever to grope the sample surface, thus determining its topology. One of the main advantages of the AFM compared to SEM is that the sample is not needed to be conductive or to be covered with thin conductive film for measurement, so it can scan almost any relatively smooth surface without sample preparation. Furthermore, the AFM can produce 3D topographic images using its basic software, with a vertical resolution of 0.02 nm and a lateral resolution of 0.1 nm, while SEM is only capable of 5 nm resolution without 3D topography. Most of the AFM can also be used in ambient air or liquid environments [13–15]. AFM is used in many scientific fields such as examination of biological samples (e.g. soil, proteins DNA…etc.) or in material science (e.g. analysis of metal alloys, semiconductors, ceramics…etc.) [16–22]. Here, it is also worth mentioning its forensic application, where many different type of material residues can be examined with this technique. That is why AFM gained ground in traditional forensic sciences as well, applicable to the examination of blood and human hair samples, damaged SIM cards, remains of packaging stuff, documents or explosive materials [23]. Although plenty of materials science studies have already been conducted with AFM on uranium, thorium thin layers and plutonium surfaces, the application of the technique for nuclear forensic purposes is very limited in the available literature [24–26]. Richard Scot Peeke's report may be mentioned who the debris of atomic explosion for nuclear forensic purposes by AFM [26].

Based on the advantages of AFM technique, such as simplicity and cost effectiveness, as well as its applicability for forensic science, AFM could be an alternative analytical technique for nuclear forensic purposes to SEM. As it was rarely used for nuclear forensic examination reported in the available literature, the purpose of this study is to investigate the applicability of AFM in nuclear forensic examination together with comparison of AFM and SEM in the case of measurement of uranium oxide fuel pellet samples.

Experimental

In this study, nine different uranium oxide fuel pellets were analysed by both SEM and AFM techniques. Among the pellets, there were reference materials with known production technology originating from international round robin exercises (e.g. Collaborating Material Exercise (CMX) organised by the Nuclear Forensics International Technical Working Group (ITWG)), as well as real confiscated nuclear fuel pellets with known measurement data using other techniques.

The samples examined are in a range of different uranium isotopic composition. The data of the samples are given in Table 1.

The examined samples had different physical characteristics, from which one can track back to different manufacturing technologies (Fig. 1). We have found that:

- NPF-1, NPF-2, NPF-4, NPF-8 pellets were produced for research purposes,
- NFP-5, NFP-6 samples resemble to pellets typical for pressurised heavy-water reactors,
- NFP-3, NFP-7, NFP-9 samples are similar to the pellets for pressurised water reactors.

Table 1 Isotopic and chemical composition of the nuclear fuel pellets (NFP), among them those having the same chemical compositions but different origin for SEM and AFM measurements

Sample ID	Sample origin*	Isotope enrichment**	Phase composition***
NFP-1	ITWG round robin exercise (CMX4)	LEU (2.19%)	UO_2, U_3O_8
NFP-2	ITWG round robin exercise (CMX4)	LEU (2.9%)	UO_2
NFP-3	ITWG round robin exercise (CMX5)	LEU (4.3%)	UO_2
NFP-4	ITWG round robin exercise (CMX5)	LEU (4.3%)	UO_2
NFP-5	Confiscated by authorities	NU	UO_2
NFP-6	Confiscated by authorities	NU	UO_2
NFP-7	Confiscated by authorities	LEU (Reproc. 2.6%)	UO_2
NFP-8	Confiscated by authorities	DU (0.23%)	UO_2, $UO_3{\cdot}2H_2O$
NFP-9	Confiscated by authorities	LEU (1.9%)	UO_2

*Please note, that the origin of samples cannot be given specifically for security reasons.

**NU: Natural Uranium, LEU: Low Enriched Uranium, DU: Diluted Uranium.

***Phase composition were determined by X-ray Diffraction Analysis (XRD).

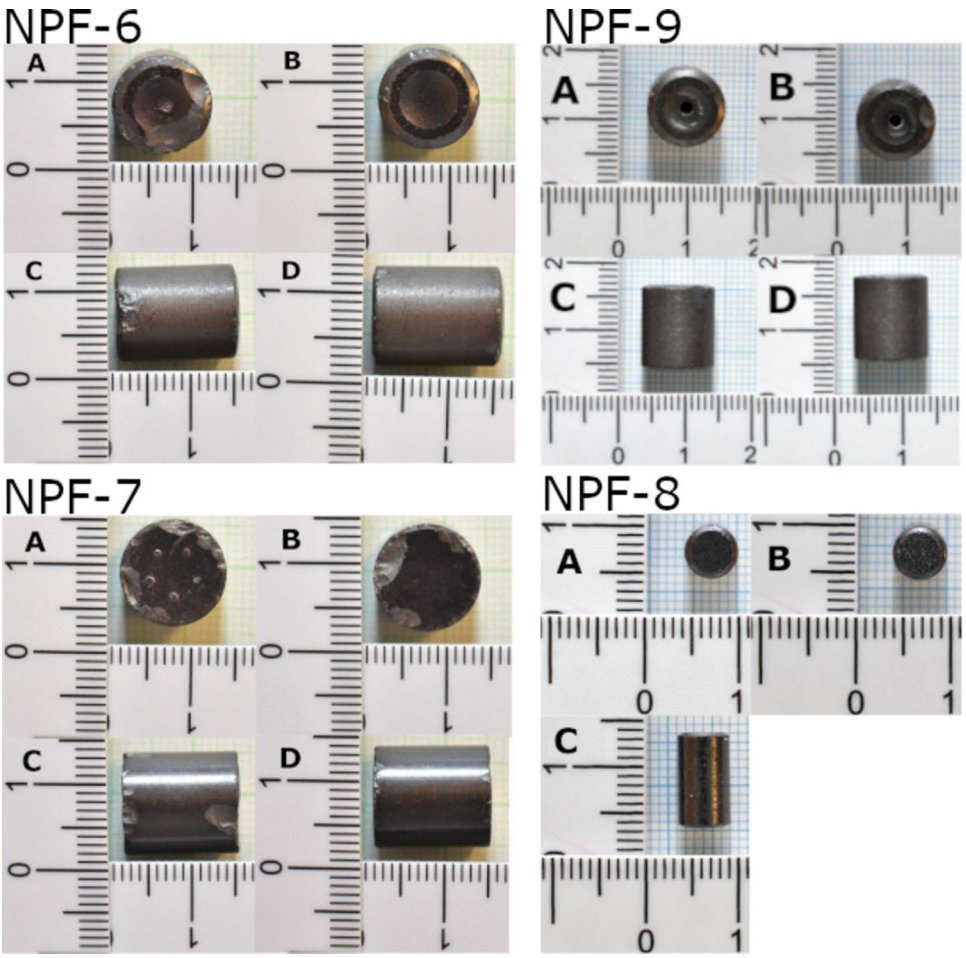

Fig. 1 Different physical characteristics of the examined samples (**A**, **B**–rear ends of the pellets; **C**, **D**–mantle of the pellets)

No special sample preparation (including the coating) was needed for the SEM and AFM measurements of the samples, because the uranium fuel pellets are solid materials, they are not pulverised and based on experience, they are not charged by the electron beam.

Images of the samples were collected on a LEO 1540 XB SEM using accelerating voltages of 5 kV. During the SEM measurements, the ESPIRIT 1.9 software was used for imaging. In case of the AFM measurements an AIST-NT SPM SmarsSPM™-1000 device was used in tapping/semi-contact mode with probe oscillation amplitude of 150 nm. The type of AFM tip used for scanning was PPP-NCHR AFM probe with 42 N/m spring constant. The images were taken at 0.4 Hz scanning rate. Five points were examined on each side of the fuel pellets.

Results and discussion

In the SEM images, on the surfaces of the samples, two different structural formations were identified, which are characteristic for the UO_2 nuclear fuel pellets: smooth featureless grains and facetted grains showing surface steps or areas. Though these morphological features of the UO_2 thin films are well known in the scientific literature on material science, these characteristics were never examined for nuclear forensic purposes [27, 28]. Based on the literature the smooth featureless grains can be assigned to the stoichiometric form of UO_2 and the facetted grains are the hyper-stoichiometric form of UO_2 [29].

During the present study the stoichiometric form was identified only on the sample surface in the case of the NFP-1, NFP-4, NFP-5, NFP-6, NFP-7 and NFP-8 samples. In the case of samples NFP-2, NFP-3 and NFP-9 a mixture of both stoichiometric and hyper-stoichiometric forms were observed. These samples were analysed by AFM at 2 sides in 5 points (10 measurement points/sample) and hyper-stoichiometric form was found in every image consequently. From these three samples two of them (NFP-2, NFP-3) are produced for scientific purposes (exercises) and not commercial nuclear fuel pellets used in reactors. See an example in Fig. 2. Long term storage or storage conditions cannot be the origin of the hyper-stoichiometric form as NFP-5, NFP-6, NFP-7 and NFP-8 samples were produced much earlier than NFP-2 and NFP-3, while the production date of the NFP-9 is close to samples mentioned above The production date of the samples was determined by mass-spectrometry at our institution. All these samples were stored under the same conditions.

As the hyper-stoichiometric forms can be found only in certain nuclear fuel pellets it can indicate different production technology of these pellets. In the followings this difference will be demonstrated via the analysis of two reference materials with known production technology originating from the same round robin exercise. The physical characteristics such as fine and large macrostructure of the samples can already be seen during visual inspection and under the optical microscope. The microscopic images are demonstrated in Fig. 3.

Based on Fig. 3 the NFP-3 sample is a compact, dense, well-formed pellet with specific surface shape characteristics, such as edges and lenses on the bottom and the top area of the pellet. However, the NFP-4 sample is clearly different, it contains large and rough grains, the surface is not smooth and there are no specific shape characteristics. The bottom and the top parts of the pellet are flat. So obviously the fuel fabrication procedure is different, as it is known from the round robin exercise description. The UO_2 raw material of the pellets were manufactured by the integral dry route preparation, dry sintering. Two very different macrostructures were created. In the case of NFP-4 sample 0.8 wt%

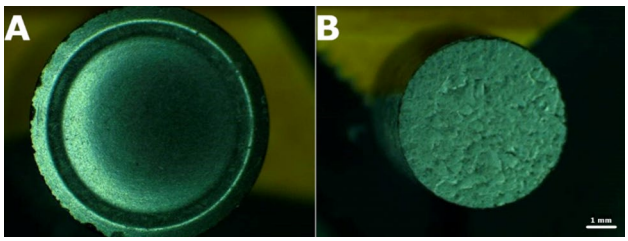

Fig. 3 Optical microscope images of NFP-3 (**A**), NFP-4 (**B**)

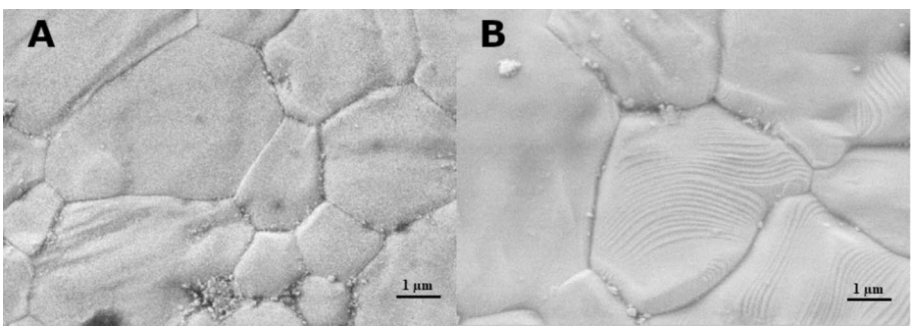

Fig. 2 SEM images showing stoichiometric form on NFP-5 (**A**) and the hyper-stoichiometric form on NFP-2 (**B**)

pore-maker was mixed to raw material 50 MPa compaction pressure was used for NFP-3 and definite grain size (160 µm) was obtained by sieving/forcing before formatting compaction (450 MPa) and sintering. 600 MPa compaction pressure was utilised for NFP-4, however in this case larger grain size (800 µm) was obtained from Forced sieving and used for preparation of soft mix before formatting compaction (400 MPa) and sintering. Sintering was carried out in pure H_2 atmosphere, in 1700 °C, 4 h long.

Based on the open literature, the most common reason for formation of the hyper-stoichiometric surface morphology in uranium is the application of low temperature and/or not inert atmosphere such as hydrogen during flash sintering process. Especially, using H_2 atmosphere the interstitial oxygen can diffuse easily to the material and is able to formulate different stoichiometric uranium-oxide forms. However, in the case of the NFP-3 and NFP-4 samples the parameters of the sintering procedure are the same (1700 °C during 4 h in pure H_2 atmosphere), the hyper-stoichiometric form can be found only on the surface of the NFP-3 sample. The potential reason of this difference based on the information of the full production technology of the two samples (see below) is the different grain sizes formulated after compaction, during forced-sieving. The finer 160 µm grain size results in a larger total surface area of the grains that causes adsorption of oxygen in larger amounts. Thus, it is more difficult the diffusion of oxygen out from the material during the sintering process.

The samples were also analysed by AFM in order to get more detailed information on surface morphology using different type of AFM scan images, such as 3D topography and surface roughness that cannot be performed by SEM. The different stoichiometric forms seen in the SEM images appear in higher details on the AFM scan images (Fig. 4).

In order to compare SEM and AFM, first the so-called MAG type images were taken by AFM, which are similar to the SEM imaging. The MAG images show the lateral distribution of the amplitude of the probe oscillation which has highest value at the grain boundaries, steps, thus giving clearer contour of the grain boundaries. The result of this is the surface borders are drawn more contoured in the case of uranium fuel pellets. Therefore, with the examination of the MAG together with 3D topographic scans, the hyper-stoichiometric form can be certainly identified and cannot be mixed with other surface effects. Based on the morphological analysis of the pellet by SEM and AFM, the morphological differences of the samples identified using both microscopic techniques, however using AFM with the 3D topographic scan mode, more detailed morphological information can be obtained comparing with SEM technique (Fig. 5).

All the other analysed samples were also scanned by AFM. MAG images of four other samples can be seen in Fig. 6.

Another analysing tool to compare the two techniques is the grain size distribution. Based on both SEM images and AFM scans, the grain size distributions can be determined. The comparison of grain size distribution calculated from SEM and AFM measurements is demonstrated in Fig. 7. For these calculations the same area of the NFP-3 and NFP-4 samples were scanned both by SEM and AFM. As it can be seen, the two techniques gave similar results. NFP-3 and NFP-4 samples were both analysed for grain size distribution on the same scanning area but significant differences in the grain size was not found, as was expected. Both SEM and AFM can provide similar results however, they are using different scanning methodology. The differences between the two samples can

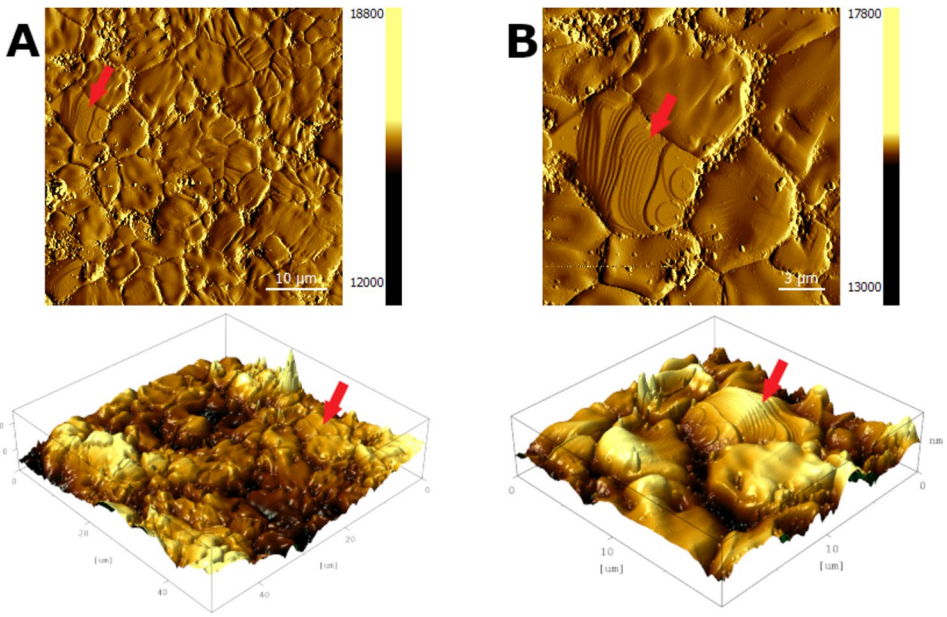

Fig. 4 The MAG type and 3D topographic image of hyper-stoichiometric form (Red arrow) of UO_2 in the surface of sample NFP-9 by AFM (**A**: 50×50 µm; **B**: 20×20 µm)

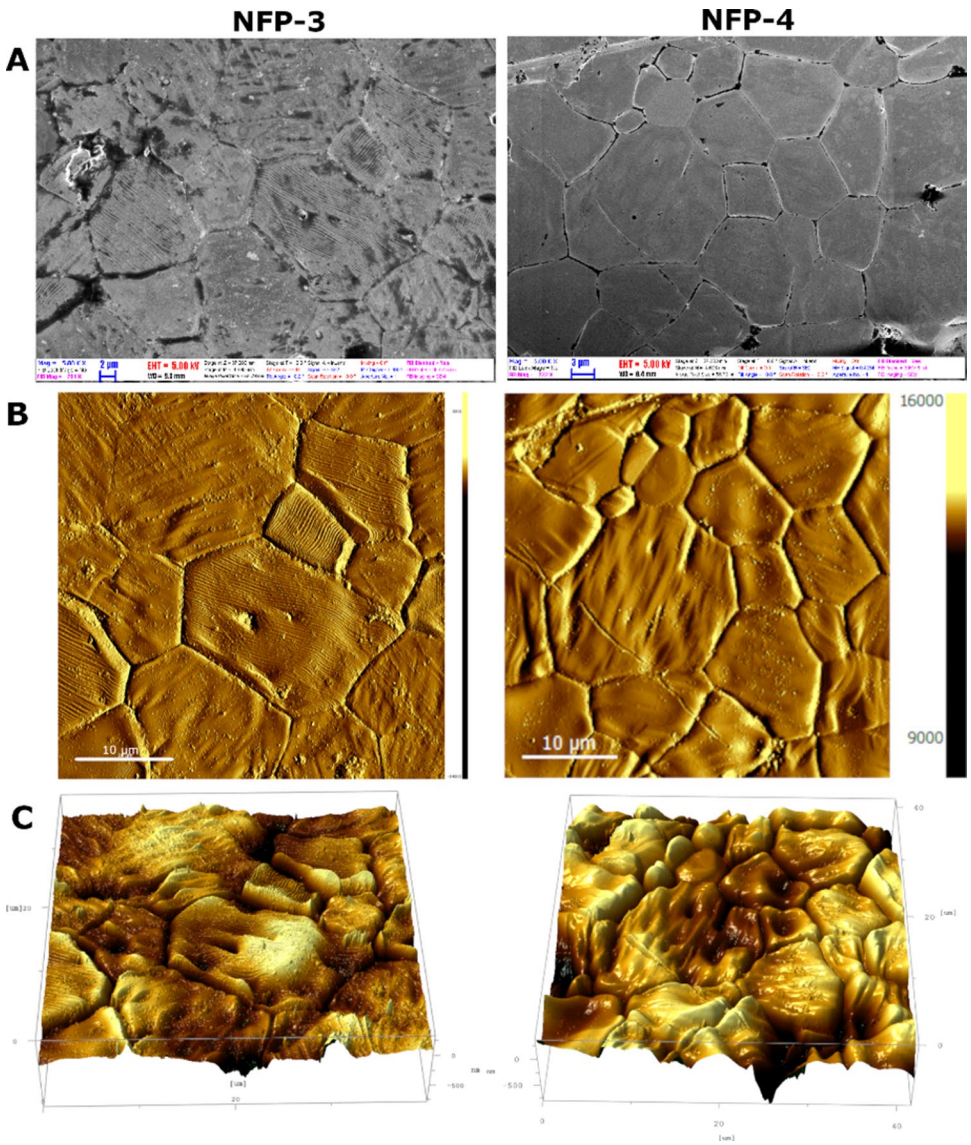

Fig. 5 SEM (**A**), AFM MAG (**B**) and 3D (**C**) images of NFP-3 and NFP-4 samples from the same spot

be seen in the grain size. The most common diameter of the particles can be found at the NFP-3 sample are between 10 and 12 µm and for NFP-4 samples between 6 and 14 µm. It confirms that the NFP-3 sample material is more homogeneous.

Furthermore, contrary to the SEM, using the AFM, the surface roughness of the pellets can also be examined, which allowed to analyse another characteristic parameter of the samples. However, in this case comparing the grain size distribution and surface roughness of the stoichiometric and hyper-stoichiometric form pellets, no significant differences were found (Fig. 8).

Conclusions

Based on the results presented, it can be concluded that similarly to SEM measurements, AFM is also capable to provide information about the morphology of nuclear fuel pellets, however with higher resolution. As an advantage the SEM equipped with Energy Dispersive X-ray Spectroscopy (EDX) is useful for semi-quantitative elemental analysis and elemental mapping. On the other hand, the AFM is also capable to produce 3D-topographic images,

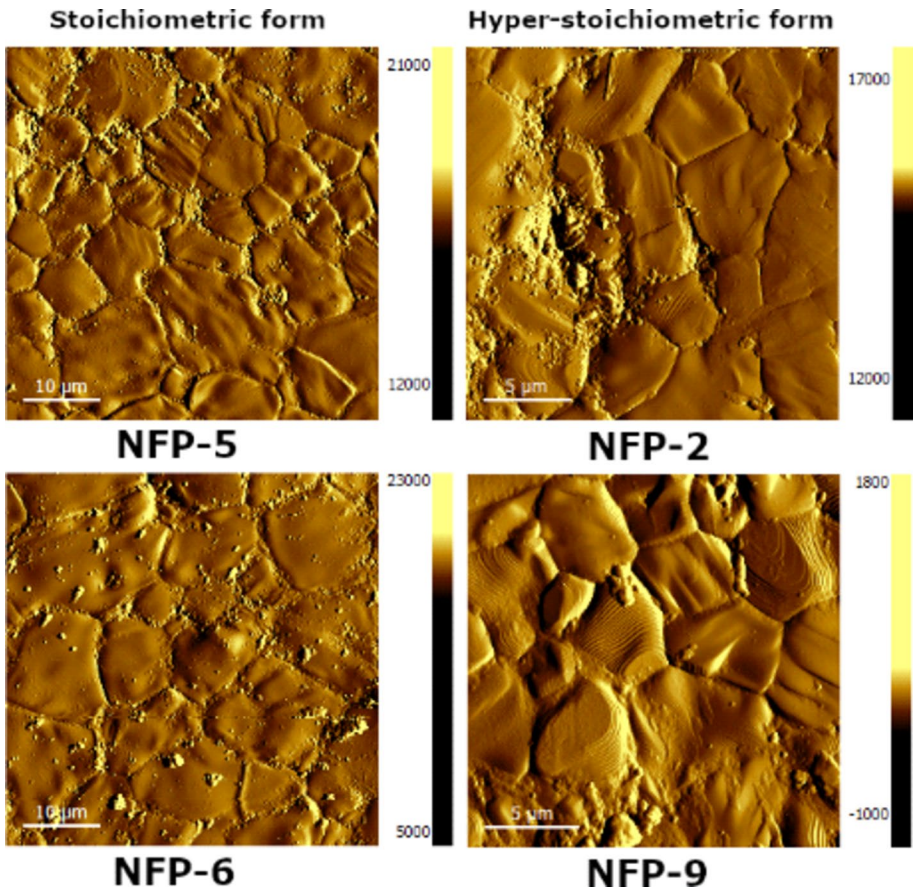

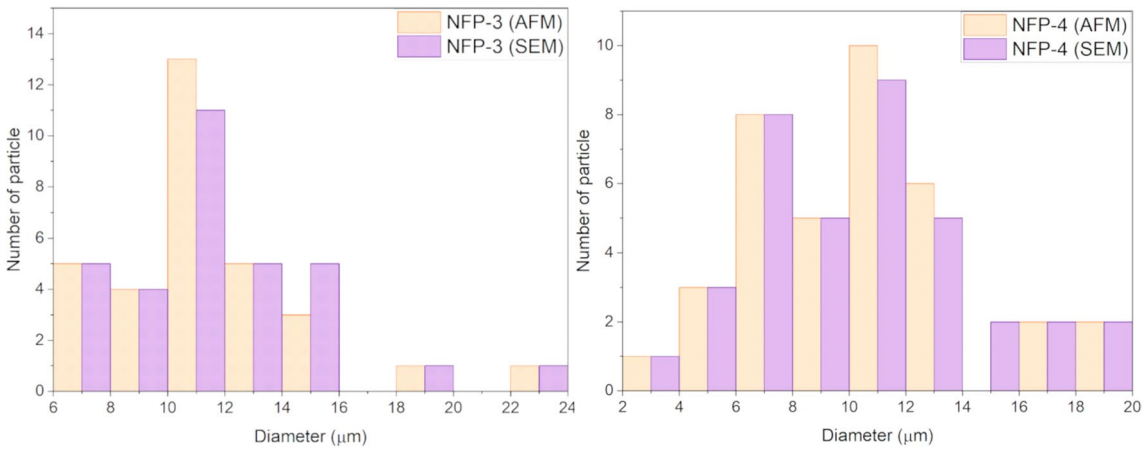

Fig. 6 Examples of stoichiometric and hyper-stoichiometric form among the samples

Fig. 7 Grain size distribution of NFP-3 and NFP-4 samples measured by AFM and SEM

that can be useful for calculation of grain size distribution and measurement of the surface roughness. Furthermore, the AFM is also capable to identify the different material components (phases). In summary the AFM provides morphological data similar to SEM, so it can be suitable as an additional microscopic technique to morphological study for nuclear forensic examinations. The main advantage of the AFM compared to SEM is that it is a cost effective, simpler to operate technique and additionally it is capable to produce 3D-topographic model of the surface of the samples that gives more tools for forensic examination.

Based on the morphological analysis of more nuclear fuel pellets with different production technology, a characteristic parameter of fuel pellets was identified, i.e. the hyper-stoichiometric form of UO_2. This form was found only in certain fuel pellets. It means that the hyper-stoichiometric form

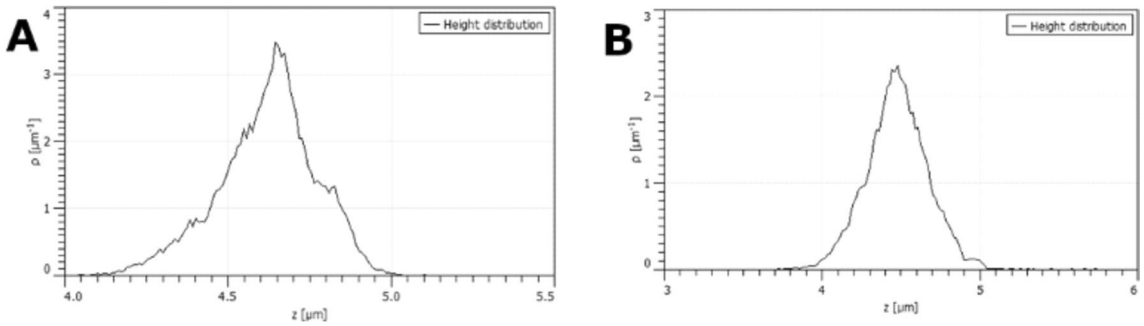

Fig. 8 Height distribution of NFP-8 (**A**) and NFP-9 (**B**) samples

does not occurred random, it can indicate differences in the parameters of the sintering process or in this study different grain size used for pellet production. That can identify the production technology and in such way to identify or exclude producers or differentiate samples. In conclusion, the hyper-stoichiometric form of nuclear materials was found as a possible novel signature in origin assessment to nuclear forensic examination.

Acknowledgements The work was performed in the framework of the Hevesy György Ph.D. School for Chemistry, Eötvös Loránd University, Budapest, Hungary. Levente Illés and Zoltán Kovács from Institute of Technical Physics and Materials Sciences, HUN-REN Centre for Energy Research for the SEM measurements.

Funding Open access funding provided by Eötvös Loránd University.

Data availability The authors declare that the data supporting the findings of this study are available within the paper and its Supplementary Information files. Should any raw data files be needed in another format they are available from the corresponding author upon reasonable request.

Declarations

Conflict of interest The authors declare that they have no known competing financial interests or personal relationships that could have appeared to influence the work reported in this paper.

References

1. IAEA Nuclear Security Series No. 2-G (2015) Nuclear forensics in support of investigation. IAEA, Vienna
2. Lützenkirchen K, Wallenius M, Varga Z, Wiss T, Knott A, Nicholl A, Mayer K (2019) Nuclear forensics on uranium fuel pellets. Radiochim Acta 107:635–643. https://doi.org/10.1515/ract-2018-3068
3. Cordfunke EHP, van der Giessen A (1967) A Particle properties and sintering behaviour of uranium dioxide. J Nucl Mater 24:141–149. https://doi.org/10.1016/0022-3115(67)90002-5
4. Olsen AM, Richards B, Schwerdt I, Heffernan S, Robert L, Smith B, Jurrus E, Ruggiero C, McDonald LW IV (2017) Quantifying morphological features of α-U3O8 with image analysis for nuclear forensics. Anal Chem 89:3177–3183. https://doi.org/10.1021/acs.analchem.6b05020
5. Tamasi AL, Cash LJ, Mullen TW, Pugmire LA, Ross AR, Ruggiero CE, Scott BL, Wagner GL, Walensky JR, Wilkerson MP (2017) Morphology of U_3O_8 materials following storage under controlled conditions of temperature and relative humidity. J Radioanal Nucl Chem 311:35–42. https://doi.org/10.1007/s10967-016-4923-1
6. Ly C, Olsen AM, Schwerdt IJ, Porter R, Sentz K, McDonald LW IV, Tasdizen T (2019) A new approach for quantifying morphological features of U_3O_8 for nuclear forensics using a deep learning model. J Nucl Mater 517:128–137. https://doi.org/10.1016/j.jnucmat.2019.01.042
7. Manara D, Renker B (2003) Raman spectra of stoichiometric and hyperstochiometric uranium dioxide. J Nucl Mater 321:233–237. https://doi.org/10.1016/S0022-3115(03)00248-4
8. Guéneau C, Baichi M, Labroche D, Chatillon C, Sundman B (2002) Thermodynamic assessment of the uranium-oxygen system. J Nucl Mater 304:161–175. https://doi.org/10.1016/S0022-3115(02)00878-4
9. Wang J, Ewing RC, Becker U (2014) Average structure and local configuration of excess oxygen in UO_{2+x}. Sci Rep 4:4216. https://doi.org/10.1038/srep04216
10. Moody KJ, Grant PM, Hutcheon ID (2014) Nuclear forensic analysis. CRC Press
11. Nizinski CA, Hanson AB, Fullmer BC, Mecham NJ, Tasdizen T, McDonald LW IV (2020) Effects of process history on the surface morphology of uranium ore concentrates extracted from ore. Miner Eng 156:106457. https://doi.org/10.1016/j.mineng.2020.106457
12. Nerikar PV, Rudman K, Desai TG, Byler D, Unal C, McClellan KJ, Phillpot SR, Sinnott SB, Peralta P, Uberuaga BP, Stanek CR, Grain, (2011) Boundaries in uranium dioxide: scanning

electron microscopy experiments and atomistic simulations. J Am Ceram Soc 94:1893–1900
13. Meyer E (1992) Atomic force microscopy. Prog Surf Sci 41:3–49. https://doi.org/10.1016/0079-6816(92)90009-7
14. Giessibl FJ (2003) Advances in atomic force microscopy. Rev Mod Phys 75:949. https://doi.org/10.1103/RevModPhys.75.949
15. Pand G, Tharmavaram M, Rawtani D, Kumar S, Agrawal Y (2017) Multifarious applications of atomic force microscopy in forensic science investigations. Forensic Sci Int 273:53–63. https://doi.org/10.1016/j.forsciint.2017.01.030
16. Cheng S, Bryant R, Doerr SH, Rhodri Williams P, Wright CJ (2008) Application of atomic force microscopy to the study of natural and model soil particles. J Microsc 231:384–394. https://doi.org/10.1111/j.1365-2818.2008.02051.x
17. Pleshakova TO, Bukharina NS, Archakov AI, Ivanov YD (2018) Atomic force microscopy for protein detection and their physicochemical characterization. Int J Mol Sci 19:1142. https://doi.org/10.3390/ijms19041142
18. Hansma HG (2001) Surface biology of DNA by atomic force microscopy. Annu Rev Phys Chem 52:71–92. https://doi.org/10.1146/annurev.physchem.52.1.71
19. Valois CRA, Silva LP, Azevedo RB (2005) Atomic force microscopy study of stainless-steel and nickel-titanium files. J Endod 31:882–885. https://doi.org/10.1097/01.don.0000164132.27285.2c
20. Oyabu N, Sugimoto Y, Abe M, Custance O, Morita S (2005) Lateral manipulation of single atoms at semiconductor surfaces using atomic force microscopy. Nanotechnology 16:S112. https://doi.org/10.1088/0957-4484/16/3/021
21. Fattahi M, Nezafat NB, Talu S, Solaymani S, Ghoranneviss M, Elahi SM, Shafiekhani A, Rezaee S (2020) Topographic characterization of zirconia-based ceramics by atomic force microscopy: a case study on different laser irradiations. J Alloy Compd 831:154763. https://doi.org/10.1016/j.jallcom.2020.154763
22. Shukla RK, Kapoor N, Badiye A (2022) Forensic microscopy: truth under the lenses. CRC Press, Boca Raton
23. Sadi S, Paulenova A, Watson PR, Loveland W (2011) Growth and surface morphology of uranium films during molecular plating. Nucl Instrum Method Phys Res, Sect A 655:80–84. https://doi.org/10.1016/j.nima.2011.06.025
24. Mahmoud SA (2002) Characterization of thorium dioxide thin films prepared by the spray pyrolysis technique. Solid State Sci 4:221–228. https://doi.org/10.1016/S1293-2558(01)01229-8
25. Beaux MF, Peterson RJ, Usov IO (2021) Topographic and nanomechanical mapping of plutonium surfaces. Surf Interfaces 26:101382. https://doi.org/10.1016/j.surfin.2021.101382
26. Peeke RS (2014) Exploring a novel approach to technical nuclear forensics utilizing atomic force microscopy. Dissertations, theses, and masters projects. Paper 1539626950. https://doi.org/10.21220/s2-6apc-yy11
27. He H, Ding Z, Shoesmith DW (2009) The determination of electrochemical reactivity and sustainability on individual hyper-stoichiometric UO2+x grains by Raman microspectroscopy and scanning electrochemical microscopy. Electrochem Commun 11:1724–1727. https://doi.org/10.1016/j.elecom.2009.07.013
28. He H, Zhu RK, Qin Z, Keech P, Ding Z, Shoesmith DW (2009) Determination of local corrosion kinetics on hyper-stoichiometric UO2+x by scanning electrochemical microscopy. J Electrochem Soc 156(3):C87. https://doi.org/10.1149/1.3046112
29. O'Neil KD, He H, Keech P, Shoesmith DW, Semenikhin OA (2008) Anisotropy of local electrical conductivity of hyper-stoichiometric uranium dioxide revealed by current-sensing atomic force microscopy (CS-AFM). Electrochem Commun 10:1805–1808. https://doi.org/10.1016/j.elecom.2008.09.009